

## Chapter 27

# Irrationally winding

I don't care for islands, especially very small ones.

—D.H. Lawrence

(R. Artuso and P. Cvitanović)

**T**HIS CHAPTER is concerned with the mode locking problems for circle maps: besides its physical relevance it nicely illustrates the use of cycle expansions away from the dynamical setting, in the realm of renormalization theory at the transition to chaos.

The physical significance of circle maps is connected with their ability to model the two-frequencies mode-locking route to chaos for dissipative systems. In the context of *dissipative* dynamical systems one of the most common and experimentally well explored routes to chaos is the two-frequency mode-locking route. Interaction of pairs of frequencies is of deep theoretical interest due to the generality of this phenomenon; as the energy input into a dissipative dynamical system (for example, a Couette flow) is increased, typically first one and then two of intrinsic modes of the system are excited. After two Hopf bifurcations (a fixed point with inward spiralling stability has become unstable and outward spirals to a limit cycle) a system lives on a two-torus. Such systems tend to mode-lock: the system adjusts its internal frequencies slightly so that they fall in step and minimize the internal dissipation. In such case the ratio of the two frequencies is a rational number. An irrational frequency ratio corresponds to a quasiperiodic motion - a curve that never quite repeats itself. If the mode-locked states overlap, chaos sets in. The likelihood that a mode-locking occurs depends on the strength of the coupling of the two frequencies.

Our main concern in this chapter is to illustrate the “global” theory of circle maps, connected with universality properties of the whole irrational winding set. We shall see that critical global properties may be expressed via cycle expansions involving “local” renormalization critical exponents. The renormalization theory of critical circle maps demands rather tedious numerical computations, and our

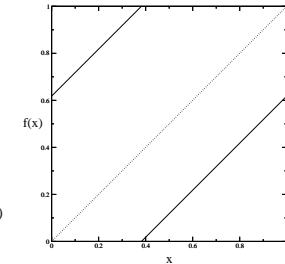


**Figure 27.1:** Unperturbed circle map ( $k = 0$  in (27.1)) with golden mean rotation number.

intuition is much facilitated by approximating circle maps by number-theoretic models. The models that arise in this way are by no means mathematically trivial, they turn out to be related to number-theoretic abyscess such as the Riemann conjecture, already in the context of the “trivial” models.

### 27.1 Mode locking

The simplest way of modeling a nonlinearly perturbed rotation on a circle is by 1-dimensional circle maps  $x \rightarrow x' = f(x)$ , restricted to the one dimensional torus, such as the *sine map*

$$x_{n+1} = f(x_n) = x_n + \Omega - \frac{k}{2\pi} \sin(2\pi x_n) \quad \text{mod } 1. \quad (27.1)$$

$f(x)$  is assumed to be continuous, have a continuous first derivative, and a continuous second derivative at the inflection point (where the second derivative vanishes). For the generic, physically relevant case (the only one considered here) the inflection is cubic. Here  $k$  parametrizes the strength of the nonlinear interaction, and  $\Omega$  is the *bare* frequency.

The state space of this map, the unit interval, can be thought of as the elementary cell of the map

$$\hat{x}_{n+1} = \hat{f}(\hat{x}_n) = \hat{x}_n + \Omega - \frac{k}{2\pi} \sin(2\pi \hat{x}_n). \quad (27.2)$$

where  $\hat{\cdot}$  is used in the same sense as in chapter 25.

The winding number is defined as

$$W(k, \Omega) = \lim_{n \rightarrow \infty} (\hat{x}_n - \hat{x}_0)/n. \quad (27.3)$$

and can be shown to be independent of the initial value  $\hat{x}_0$ .

For  $k = 0$ , the map is a simple rotation (the *shift map*) see figure 27.1

$$x_{n+1} = x_n + \Omega \pmod{1}, \tag{27.4}$$

and the rotation number is given by the parameter  $\Omega$ .

$$W(k = 0, \Omega) = \Omega.$$

For given values of  $\Omega$  and  $k$  the winding number can be either rational or irrational. For invertible maps and rational winding numbers  $W = P/Q$  the asymptotic iterates of the map converge to a unique attractor, a stable periodic orbit of period  $Q$

$$f^Q(\hat{x}_i) = \hat{x}_i + P, \quad i = 0, 1, 2, \dots, Q - 1.$$

This is a consequence of the independence of  $\hat{x}_0$  previously mentioned. There is also an unstable cycle, repelling the trajectory. For any rational winding number, there is a finite interval of values of  $\Omega$  values for which the iterates of the circle map are attracted to the  $P/Q$  cycle. This interval is called the  $P/Q$  *mode-locked* (or *stability*) interval, and its width is given by exercise 27.1

$$\Delta_{P/Q} = Q^{-2\mu_{P/Q}} = \Omega_{P/Q}^{right} - \Omega_{P/Q}^{left}. \tag{27.5}$$

where  $\Omega_{P/Q}^{right}$  ( $\Omega_{P/Q}^{left}$ ) denote the biggest (smallest) value of  $\Omega$  for which  $W(k, \Omega) = P/Q$ . Parametrizing mode lockings by the exponent  $\mu$  rather than the width  $\Delta$  will be convenient for description of the distribution of the mode-locking widths, as the exponents  $\mu$  turn out to be of bounded variation. The stability of the  $P/Q$  cycle is

$$\Lambda_{P/Q} = \frac{\partial x_Q}{\partial x_0} = f'(x_0)f'(x_1)\cdots f'(x_{Q-1})$$

For a stable cycle  $|\Lambda_{P/Q}|$  lies between 0 (the superstable value, the “center” of the stability interval) and 1 (the  $\Omega_{P/Q}^{right}$ ,  $\Omega_{P/Q}^{left}$  endpoints of (27.5)). For the shift map (27.4), the stability intervals are shrunk to points. As  $\Omega$  is varied from 0 to 1, the iterates of a circle map either mode-lock, with the winding number given by a rational number  $P/Q \in (0, 1)$ , or do not mode-lock, in which case the winding number is irrational. A plot of the winding number  $W$  as a function of the shift parameter  $\Omega$  is a convenient visualization of the mode-locking structure of circle maps. It yields a monotonic “devil’s staircase” of figure 27.2 whose self-similar structure we are to unravel. Circle maps with zero slope at the inflection point  $x_c$  (see figure 27.3)

$$f'(x_c) = 0, \quad f''(x_c) = 0$$

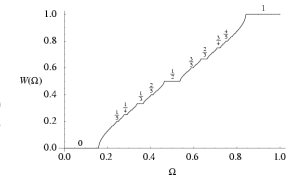


Figure 27.2: The critical circle map ( $k = 1$  in (27.1)) devil’s staircase [27.3]; the winding number  $W$  as function of the parameter  $\Omega$ .

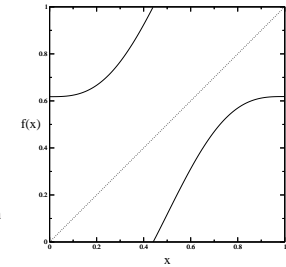


Figure 27.3: Critical circle map ( $k = 1$  in (27.1)) with golden mean bare rotation number.

( $k = 1$ ,  $x_c = 0$  in (27.1)) are called *critical*: they delineate the borderline of chaos in this scenario. As the nonlinearity parameter  $k$  increases, the mode-locked intervals become wider, and for the critical circle maps ( $k = 1$ ) they fill out the whole interval. A critical map has a superstable  $P/Q$  cycle for any rational  $P/Q$ , as the stability of any cycle that includes the inflection point equals zero. If the map is non-invertible ( $k > 1$ ), it is called *supercritical*; the bifurcation structure of this regime is extremely rich and beyond the scope of this exposition.

The physically relevant transition to chaos is connected with the critical case, however the apparently simple “free” shift map limit is quite instructive: in essence it involves the problem of ordering rationals embedded in the unit interval on a hierarchical structure. From a physical point of view, the main problem is to identify a (number-theoretically) consistent hierarchy susceptible of experimental verification. We will now describe a few ways of organizing rationals along the unit interval: each has its own advantages as well as its drawbacks, when analyzed from both mathematical and physical perspective.

### 27.1.1 Hierarchical partitions of the rationals

Intuitively, the longer the cycle, the finer the tuning of the parameter  $\Omega$  required to attain it; given finite time and resolution, we expect to be able to resolve cycles up to some maximal length  $Q$ . This is the physical motivation for partitioning mode lockings into sets of cycle length up to  $Q$ . In number theory such sets of rationals are called *Farey series*. They are denoted by  $\mathcal{F}_Q$  and defined as follows. The Farey series of order  $Q$  is the monotonically increasing sequence of all irreducible rationals between 0 and 1 whose denominators do not exceed  $Q$ . Thus  $P_i/Q_i$

belongs to  $\mathcal{F}_Q$  if  $0 < P_i \leq Q_i \leq Q$  and  $(P_i|Q_i) = 1$ . For example

$$\mathcal{F}_5 = \left\{ \frac{1}{5}, \frac{1}{4}, \frac{1}{3}, \frac{2}{5}, \frac{1}{2}, \frac{3}{5}, \frac{2}{3}, \frac{3}{4}, \frac{4}{5}, \frac{1}{1} \right\}$$

A Farey series is characterized by the property that if  $P_{i-1}/Q_{i-1}$  and  $P_i/Q_i$  are consecutive terms of  $\mathcal{F}_Q$ , then

$$P_i Q_{i-1} - P_{i-1} Q_i = 1.$$

The number of terms in the Farey series  $F_Q$  is given by

$$\Phi(Q) = \sum_{n=1}^Q \phi(Q) = \frac{3Q^2}{\pi^2} + O(Q \ln Q). \tag{27.6}$$

Here the Euler function  $\phi(Q)$  is the number of integers not exceeding and relatively prime to  $Q$ . For example,  $\phi(1) = 1, \phi(2) = 1, \phi(3) = 2, \dots, \phi(12) = 4, \phi(13) = 12, \dots$

From a number-theorist's point of view, the *continued fraction partitioning* of the unit interval is the most venerable organization of rationals, preferred already by Gauss. The continued fraction partitioning is obtained by ordering rationals corresponding to continued fractions of increasing length. If we turn this ordering into a way of covering the complementary set to mode-lockings in a circle map, then the first level is obtained by deleting  $\Delta_{[1]}, \Delta_{[2]}, \dots, \Delta_{[a_1]}, \dots$  mode-lockings; their complement are the *covering* intervals  $\ell_1, \ell_2, \dots, \ell_{a_1}, \dots$  which contain all windings, rational and irrational, whose continued fraction expansion starts with  $[a_1, \dots]$  and is of length at least 2. The second level is obtained by deleting  $\Delta_{[1,2]}, \Delta_{[1,3]}, \dots, \Delta_{[2,2]}, \Delta_{[2,3]}, \dots, \Delta_{[n,m]}, \dots$  and so on.

The  $n$ th level continued fraction partition  $S_n = \{a_1 a_2 \dots a_n\}$  is defined as the monotonically increasing sequence of all rationals  $P_i/Q_i$  between 0 and 1 whose continued fraction expansion is of length  $n$ :

$$\frac{P_i}{Q_i} = [a_1, a_2, \dots, a_n] = \frac{1}{a_1 + \frac{1}{a_2 + \dots + \frac{1}{a_n}}}$$

The object of interest, the set of the irrational winding numbers, is in this partitioning labeled by  $S_\infty = \{a_1 a_2 a_3 \dots\}$ ,  $a_k \in \mathbb{Z}^+$ , i.e., the set of winding numbers with infinite continued fraction expansions. The continued fraction labeling is particularly appealing in the present context because of the close connection of the Gauss

shift to the renormalization transformation  $R$ , discussed below. The Gauss map

$$T(x) = \begin{cases} \frac{1}{x} - \left[ \frac{1}{x} \right] & x \neq 0 \\ 0, & x = 0 \end{cases} \tag{27.7}$$

( $[\dots]$  denotes the integer part) acts as a shift on the continued fraction representation of numbers on the unit interval

$$x = [a_1, a_2, a_3, \dots] \rightarrow T(x) = [a_2, a_3, \dots]. \tag{27.8}$$

into the “mother” interval  $\ell_{a_2 a_3 \dots}$ .

However natural the continued fractions partitioning might seem to a number theorist, it is problematic in practice, as it requires measuring infinity of mode-lockings even at the first step of the partitioning. Thus numerical and experimental use of continued fraction partitioning requires at least some understanding of the asymptotics of mode-lockings with large continued fraction entries.

The *Farey tree partitioning* is a systematic bisection of rationals: it is based on the observation that roughly halfway between any two large stability intervals (such as  $1/2$  and  $1/3$ ) in the devil's staircase of figure 27.2 there is the next largest stability interval (such as  $2/5$ ). The winding number of this interval is given by the Farey mediant  $(P+P')/(Q+Q')$  of the parent mode-lockings  $P/Q$  and  $P'/Q'$ . This kind of cycle “gluing” is rather general and by no means restricted to circle maps; it can be attained whenever it is possible to arrange that the  $Q$ th iterate deviation caused by shifting a parameter from the correct value for the  $Q$ -cycle is exactly compensated by the  $Q'$ th iterate deviation from closing the  $Q'$ -cycle; in this way the two near cycles can be glued together into an exact cycle of length  $Q+Q'$ . The Farey tree is obtained by starting with the ends of the unit interval written as  $0/1$  and  $1/1$ , and then recursively bisecting intervals by means of Farey mediants.

We define the  $n$ th *Farey tree level*  $T_n$  as the monotonically increasing sequence of those continued fractions  $[a_1, a_2, \dots, a_k]$  whose entries  $a_i \geq 1, i = 1, 2, \dots, k - 1, a_k \geq 2$ , add up to  $\sum_{i=1}^k a_i = n + 2$ . For example

$$T_2 = \{[4], [2, 2], [1, 1, 2], [1, 3]\} = \left( \frac{1}{4}, \frac{1}{5}, \frac{3}{5}, \frac{3}{4} \right). \tag{27.9}$$

The number of terms in  $T_n$  is  $2^n$ . Each rational in  $T_{n-1}$  has two “daughters” in  $T_n$ , given by

$$[\dots, a - 1, 2] \quad [\dots, a] \quad [\dots, a + 1]$$

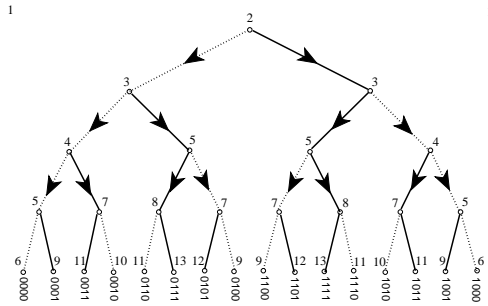


**Figure 27.4:** Farey tree: alternating binary ordered labeling of all Farey denominators on the  $n$ th Farey tree level.

Iteration of this rule places all rationals on a binary tree, labeling each by a unique binary label, figure 27.4.

The smallest and the largest denominator in  $T_n$  are respectively given by

$$[n - 2] = \frac{1}{n - 2}, \quad [1, 1, \dots, 1, 2] = \frac{F_{n+1}}{F_{n+2}} \propto \rho^n, \quad (27.10)$$


where the Fibonacci numbers  $F_n$  are defined by  $F_{n+1} = F_n + F_{n-1}$ ;  $F_0 = 0, F_1 = 1$ , and  $\rho$  is the golden mean ratio

$$\rho = \frac{1 + \sqrt{5}}{2} = 1.61803 \dots \quad (27.11)$$

Note the enormous spread in the cycle lengths on the same level of the Farey tree:  $n \leq Q \leq \rho^n$ . The cycles whose length grows only as a power of the Farey tree level will cause strong non-hyperbolic effects in the evaluation of various averages.

Having defined the partitioning schemes of interest here, we now briefly summarize the results of the circle-map renormalization theory.

### 27.2 Local theory: “Golden mean” renormalization

 The way to pinpoint a point on the border of order is to recursively adjust the parameters so that at the recurrence times  $t = n_1, n_2, n_3, \dots$  the trajectory passes through a region of contraction sufficiently strong to compensate for the accumulated expansion of the preceding  $n_i$  steps, but not so strong as to force the trajectory into a stable attracting orbit. The *renormalization operation*  $R$  implements this procedure by recursively magnifying the neighborhood of a point on the border in the dynamical space (by rescaling by a factor  $\alpha$ ), in the parameter space (by shifting the parameter origin onto the border and rescaling by a factor  $\delta$ ),

and by replacing the initial map  $f$  by the  $n$ th iterate  $f^n$  restricted to the magnified neighborhood

$$f_p(x) \rightarrow Rf_p(x) = \alpha f_{p/\delta}^n(x/\alpha)$$

There are by now many examples of such renormalizations in which the new function, framed in a smaller box, is a rescaling of the original function, i.e., the fixed point function of the renormalization operator  $R$ . The best known is the period doubling renormalization, with the recurrence times  $n_i = 2^i$ . The simplest circle map example is the golden mean renormalization, with recurrence times  $n_i = F_i$  given by the Fibonacci numbers (27.10). Intuitively, in this context a metric self-similarity arises because iterates of critical maps are themselves critical, i.e., they also have cubic inflection points with vanishing derivatives.

The renormalization operator appropriate to circle maps acts as a generalization of the Gauss shift (27.38); it maps a circle map (represented as a pair of functions  $(g, f)$ , of winding number  $[a, b, c, \dots]$  into a rescaled map of winding number  $[b, c, \dots]$ :

$$R_a \begin{pmatrix} g \\ f \end{pmatrix} = \begin{pmatrix} \alpha g^{a-1} \circ f \circ \alpha^{-1} \\ \alpha g^{a-1} \circ f \circ g \circ \alpha^{-1} \end{pmatrix}, \quad (27.12)$$

Acting on a map with winding number  $[a, a, a, \dots]$ ,  $R_a$  returns a map with the same winding number  $[a, a, \dots]$ , so the fixed point of  $R_a$  has a quadratic irrational winding number  $W = [a, a, a, \dots]$ . This fixed point has a single expanding eigenvalue  $\delta_a$ . Similarly, the renormalization transformation  $R_{a_p} \dots R_{a_2} R_{a_1} \equiv R_{a_1 a_2 \dots a_p}$  has a fixed point of winding number  $W_p = [a_1, a_2, \dots, a_p, a_1, a_2, \dots]$ , with a single expanding eigenvalue  $\delta_p$ .

For short repeating blocks,  $\delta$  can be estimated numerically by comparing successive continued fraction approximants to  $W$ . Consider the  $P_r/Q_r$  rational approximation to a quadratic irrational winding number  $W_p$  whose continued fraction expansion consists of  $r$  repeats of a block  $p$ . Let  $\Omega_r$  be the parameter for which the map (27.1) has a superstable cycle of rotation number  $P_r/Q_r = [p, p, \dots, p]$ . The  $\delta_p$  can then be estimated by extrapolating from

$$\Omega_r - \Omega_{r+1} \propto \delta_p^{-r}. \quad (27.13)$$

What this means is that the “devil’s staircase” of figure 27.2 is self-similar under magnification by factor  $\delta_p$  around any quadratic irrational  $W_p$ .

The fundamental result of the renormalization theory (and the reason why all this is so interesting) is that the ratios of successive  $P_r/Q_r$  mode-locked intervals converge to *universal* limits. The simplest example of (27.13) is the sequence of Fibonacci number continued fraction approximants to the golden mean winding number  $W = [1, 1, 1, \dots] = (\sqrt{5} - 1)/2$ .

When global problems are considered, it is useful to have at least an idea on external scaling laws for mode-lockings. This is achieved, in a first analysis, by fixing the cycle length  $Q$  and describing the range of possible asymptotics.

For a given cycle length  $Q$ , it is found that the *narrowest* interval shrinks with a power law

$$\Delta_{1/Q} \propto Q^{-3} \tag{27.14}$$

For fixed  $Q$  the *widest* interval is bounded by  $P/Q = F_{n-1}/F_n$ , the  $n$ th continued fraction approximant to the *golden mean*. The intuitive reason is that the golden mean winding sits as far as possible from any short cycle mode-locking.

The golden mean interval shrinks with a universal exponent

$$\Delta_{P/Q} \propto Q^{-2\mu_1} \tag{27.15}$$

where  $P = F_{n-1}$ ,  $Q = F_n$  and  $\mu_1$  is related to the universal Shenker number  $\delta_1$  (27.13) and the golden mean (27.11) by

$$\mu_1 = \frac{\ln|\delta_1|}{2 \ln \rho} = 1.08218\dots \tag{27.16}$$

The closeness of  $\mu_1$  to 1 indicates that the golden mean approximant mode-lockings barely feel the fact that the map is critical (in the  $k=0$  limit this exponent is  $\mu = 1$ ).

To summarize: for critical maps the spectrum of exponents arising from the circle maps renormalization theory is bounded from above by the harmonic scaling, and from below by the geometric golden-mean scaling:

$$3/2 > \mu_{m/n} \geq 1.08218\dots \tag{27.17}$$

### 27.3 Global theory: Thermodynamic averaging

Consider the following average over mode-locking intervals (27.5):

$$\Omega(\tau) = \sum_{Q=1}^{\infty} \sum_{(P/Q)=1} \Delta_{P/Q}^{-\tau} \tag{27.18}$$

The sum is over all irreducible rationals  $P/Q$ ,  $P < Q$ , and  $\Delta_{P/Q}$  is the width of the parameter interval for which the iterates of a critical circle map lock onto a cycle of length  $Q$ , with winding number  $P/Q$ .

The qualitative behavior of (27.18) is easy to pin down. For sufficiently negative  $\tau$ , the sum is convergent; in particular, for  $\tau = -1$ ,  $\Omega(-1) = 1$ , as for the critical circle maps the mode-lockings fill the entire  $\Omega$  range [27.11]. However, as  $\tau$  increases, the contributions of the narrow (large  $Q$ ) mode-locked intervals  $\Delta_{P/Q}$  get blown up to  $1/\Delta_{P/Q}^\tau$ , and at some critical value of  $\tau$  the sum diverges. This occurs for  $\tau < 0$ , as  $\Omega(0)$  equals the number of all rationals and is clearly divergent.

The sum (27.18) is infinite, but in practice the experimental or numerical mode-locked intervals are available only for small finite  $Q$ . Hence it is necessary to split up the sum into subsets  $S_n = \{i\}$  of rational winding numbers  $P_i/Q_i$  on the “level”  $n$ , and present the set of mode-lockings hierarchically, with resolution increasing with the level:

$$\bar{Z}_n(\tau) = \sum_{i \in S_n} \Delta_i^{-\tau} \tag{27.19}$$

The original sum (27.18) can now be recovered as the  $z = 1$  value of a “generating” function  $\Omega(z, \tau) = \sum_n z^n \bar{Z}_n(\tau)$ . As  $z$  is anyway a formal parameter, and  $n$  is a rather arbitrary “level” in some *ad hoc* partitioning of rational numbers, we bravely introduce a still more general,  $P/Q$  weighted generating function for (27.18):

$$\Omega(q, \tau) = \sum_{Q=1}^{\infty} \sum_{(P/Q)=1} e^{-q\nu_{P/Q}} Q^{2\tau\mu_{P/Q}} \tag{27.20}$$

The sum (27.18) corresponds to  $q = 0$ . Exponents  $\nu_{P/Q}$  will reflect the importance we assign to the  $P/Q$  mode-locking, i.e., the *measure* used in the averaging over all mode-lockings. Three choices of of the  $\nu_{P/Q}$  hierarchy that we consider here correspond respectively to the Farey series partitioning

$$\Omega(q, \tau) = \sum_{Q=1}^{\infty} \Phi(Q)^{-q} \sum_{(P/Q)=1} Q^{2\tau\mu_{P/Q}} \tag{27.21}$$

the continued fraction partitioning

$$\Omega(q, \tau) = \sum_{n=1}^{\infty} e^{-qn} \sum_{[a_1, \dots, a_n]} Q^{2\tau\mu_{[a_1, \dots, a_n]}} \tag{27.22}$$

and the Farey tree partitioning

$$\Omega(q, \tau) = \sum_{k=n}^{\infty} 2^{-qn} \sum_{i=1}^{2^n} Q_i^{2\tau\mu_i} \ , \ Q_i/P_i \in T_n \ . \tag{27.23}$$

We remark that we are investigating a set arising in the analysis of the parameter space of a dynamical system: there is no “natural measure” dictated by dynamics, and the choice of weights reflects only the choice of hierarchical presentation.

### 27.4 Hausdorff dimension of irrational windings

A finite cover of the set irrational windings at the “ $n$ th level of resolution” is obtained by deleting the parameter values corresponding to the mode-lockings in the subset  $\mathcal{S}_n$ ; left behind is the set of complement *covering* intervals of widths

$$\ell_i = \Omega_{P_i/Q_i}^{min} - \Omega_{P_i/Q_i}^{max} . \tag{27.24}$$

Here  $\Omega_{P_i/Q_i}^{min}$  ( $\Omega_{P_i/Q_i}^{max}$ ) are respectively the lower (upper) edges of the mode-locking intervals  $\Delta_{P_i/Q_i}$  ( $\Delta_{P_i/Q_i}$ ) bounding  $\ell_i$  and  $i$  is a symbolic dynamics label, for example the entries of the continued fraction representation  $P/Q = [a_1, a_2, \dots, a_n]$  of one of the boundary mode-lockings,  $i = a_1 a_2 \dots a_n$ .  $\ell_i$  provide a finite cover for the irrational winding set, so one may consider the sum

$$Z_n(\tau) = \sum_{i \in \mathcal{S}_n} \ell_i^{-\tau} \tag{27.25}$$

The value of  $-\tau$  for which the  $n \rightarrow \infty$  limit of the sum (27.25) is finite is the *Hausdorff dimension*  $D_H$  of the irrational winding set. Strictly speaking, this is the Hausdorff dimension only if the choice of covering intervals  $\ell_i$  is optimal; otherwise it provides an upper bound to  $D_H$ . As by construction the  $\ell_i$  intervals cover the set of irrational winding with no slack, we expect that this limit yields the Hausdorff dimension. This is supported by all numerical evidence, but a proof that would satisfy mathematicians is lacking.

The physically relevant statement is that for critical circle maps  $D_H = 0.870 \dots$  is a (global) universal number.

exercise 27.2

#### 27.4.1 The Hausdorff dimension in terms of cycles

Estimating the  $n \rightarrow \infty$  limit of (27.25) from finite numbers of covering intervals  $\ell_i$  is a rather unilluminating chore. Fortunately, there exist considerably more elegant ways of extracting  $D_H$ . We have noted that in the case of the “trivial” mode-locking problem (27.4), the covering intervals are generated by iterations of the Farey map (27.37) or the Gauss shift (27.38). The  $n$ th level sum (27.25) can be approximated by  $\mathcal{L}_\tau^n$ , where

$$\mathcal{L}_\tau(y, x) = \delta(x - f^{-1}(y)) |f'(y)|^\tau$$

This amounts to approximating each cover width  $\ell_i$  by  $|df^n/dx|$  evaluated on the  $i$ th interval. We are thus led to the following determinant

$$\det(1 - z\mathcal{L}_\tau) = \exp\left(-\sum_p \sum_{r=1}^{\infty} \frac{z^{rp}}{r} \frac{|\Lambda_p^r|^\tau}{1 - 1/\Lambda_p^r}\right)$$

$$= \prod_p \prod_{k=0}^{\infty} \left(1 - z^{kp} |\Lambda_p^k|^\tau / \Lambda_p^k\right) . \tag{27.26}$$

The sum (27.25) is dominated by the leading eigenvalue of  $\mathcal{L}_\tau$ ; the Hausdorff dimension condition  $Z_n(-D_H) = O(1)$  means that  $\tau = -D_H$  should be such that the leading eigenvalue is  $z = 1$ . The leading eigenvalue is determined by the  $k = 0$  part of (27.26); putting all these pieces together, we obtain a pretty formula relating the Hausdorff dimension to the prime cycles of the map  $f(x)$ :

$$0 = \prod_p \left(1 - 1/|\Lambda_p|^{D_H}\right) . \tag{27.27}$$

For the Gauss shift (27.38) the stabilities of periodic cycles are available analytical, as roots of quadratic equations: For example, the  $x_a$  fixed points (quadratic irrationals with  $x_a = [a, a, a, \dots]$  infinitely repeating continued fraction expansion) are given by

$$x_a = \frac{-a + \sqrt{a^2 + 4}}{2}, \quad \Lambda_a = -\left(\frac{a + \sqrt{a^2 + 4}}{2}\right)^2 \tag{27.28}$$

and the  $x_{ab} = [a, b, a, b, a, b, \dots]$  2-cycles are given by

$$x_{ab} = \frac{-ab + \sqrt{(ab)^2 + 4ab}}{2b} \tag{27.29}$$

$$\Lambda_{ab} = (x_{ab} x_{ba})^{-2} = \left(\frac{ab + 2 + \sqrt{ab(ab + 4)}}{2}\right)^2$$

We happen to know beforehand that  $D_H = 1$  (the irrationals take the full measure on the unit interval, or, from another point of view, the Gauss map is not a repeller), so is the infinite product (27.27) merely a very convoluted way to compute the number 1? Possibly so, but once the meaning of (27.27) has been grasped, the corresponding formula for the *critical* circle maps follows immediately:

$$0 = \prod_p \left(1 - 1/|\delta_p|^{D_H}\right) . \tag{27.30}$$

The importance of this formula relies on the fact that it expresses  $D_H$  in terms of *universal* quantities, thus providing a nice connection from local universal exponents to global scaling quantities: actual computations using (27.30) are rather involved, as they require a heavy computational effort to extract Shenker’s scaling  $\delta_p$  for periodic continued fractions, and moreover dealing with an infinite alphabet requires control over tail summation if an accurate estimate is to be sought. In table 27.1 we give a small selection of computed Shenker’s scalings.

**Table 27.1:** Shenker's  $\delta_p$  for a few periodic continued fractions, from ref. [27.1].

$p$	$\delta_p$
[1 1 1 1 ...]	-2.833612
[2 2 2 2 ...]	-6.7992410
[3 3 3 3 ...]	-13.760499
[4 4 4 4 ...]	-24.62160
[5 5 5 5 ...]	-40.38625
[6 6 6 6 ...]	-62.140
[1 2 1 2 ...]	17.66549
[1 3 1 3 ...]	31.62973
[1 4 1 4 ...]	50.80988
[1 5 1 5 ...]	76.01299
[2 3 2 3 ...]	91.29055

### 27.5 Thermodynamics of Farey tree: Farey model



We end this chapter by giving an example of a number theoretical model motivated by the mode-locking phenomenology. We will consider it by means of the thermodynamic formalism of chapter K, by looking at the free energy.

Consider the Farey tree partition sum (27.23): the narrowest mode-locked interval (27.15) at the  $n$ th level of the Farey tree partition sum (27.23) is the golden mean interval

$$\Delta_{F_{n-1}/F_n} \propto |\delta_1|^{-n}. \tag{27.31}$$

It shrinks exponentially, and for  $\tau$  positive and large it dominates  $q(\tau)$  and bounds  $dq(\tau)/d\tau$ :

$$q'_{max} = \frac{\ln |\delta_1|}{\ln 2} = 1.502642 \dots \tag{27.32}$$

However, for  $\tau$  large and negative,  $q(\tau)$  is dominated by the interval (27.14) which shrinks only harmonically, and  $q(\tau)$  approaches 0 as

$$\frac{q(\tau)}{\tau} = \frac{3 \ln n}{n \ln 2} \rightarrow 0. \tag{27.33}$$

So for finite  $n$ ,  $q_n(\tau)$  crosses the  $\tau$  axis at  $-\tau = D_n$ , but in the  $n \rightarrow \infty$  limit, the  $q(\tau)$  function exhibits a phase transition;  $q(\tau) = 0$  for  $\tau < -D_H$ , but is a non-trivial function of  $\tau$  for  $-D_H \leq \tau$ . This non-analyticity is rather severe - to get a clearer picture, we illustrate it by a few number-theoretic models (the critical circle maps case is qualitatively the same).

An approximation to the "trivial" Farey level thermodynamics is given by the "Farey model," in which the intervals  $\ell_{p/Q}$  are replaced by  $Q^{-2}$ :

$$Z_n(\tau) = \sum_{i=1}^{2^n} Q_i^{2\tau}. \tag{27.34}$$

Here  $Q_i$  is the denominator of the  $i$ th Farey rational  $P_i/Q_i$ . For example (see figure 27.4),

$$Z_2(1/2) = 4 + 5 + 5 + 4.$$

By the annihilation property (27.38) of the Gauss shift on rationals, the  $n$ th Farey level sum  $Z_n(-1)$  can be written as the integral

$$Z_n(-1) = \int dx \delta(J^n(x)) = \sum 1/|f'_{a_1 \dots a_k}(0)|,$$

and in general

$$Z_n(\tau) = \int dx \mathcal{L}_\tau^n(0, x),$$

with the sum restricted to the Farey level  $a_1 + \dots + a_k = n + 2$ . It is easily checked that  $f'_{a_1 \dots a_k}(0) = (-1)^k Q_{|a_1, \dots, a_k|}^2$ , so the Farey model sum is a partition generated by the Gauss map preimages of  $x = 0$ , i.e., by rationals, rather than by the quadratic irrationals as in (27.26). The sums are generated by the same transfer operator, so the eigenvalue spectrum should be the same as for the periodic orbit expansion, but in this variant of the finite level sums we can evaluate  $q(\tau)$  exactly for  $\tau = k/2$ ,  $k$  a nonnegative integer. First, one observes that  $Z_n(0) = 2^n$ . It is also easy to check that  $Z_n(1/2) = \sum_i Q_i = 2 \cdot 3^n$ . More surprisingly,  $Z_n(3/2) = \sum_i Q^3 = 54 \cdot 7^{n-1}$ . A few of these "sum rules" are listed in the table 27.2, they are consequence of the fact that the denominators on a given level are Farey sums of denominators on preceding levels.

exercise 27.3

A bound on  $D_H$  can be obtained by approximating (27.34) by

$$Z_n(\tau) = n^{2\tau} + 2^n \rho^{2n\tau}. \tag{27.35}$$

In this approximation we have replaced all  $\ell_{p/Q}$ , except the widest interval  $\ell_{1/n}$ , by the narrowest interval  $\ell_{F_{n-1}/F_n}$  (see (27.15)). The crossover from the harmonic dominated to the golden mean dominated behavior occurs at the  $\tau$  value for which the two terms in (27.35) contribute equally:

$$D_n = \hat{D} + O\left(\frac{\ln n}{n}\right), \quad \hat{D} = \frac{\ln 2}{2 \ln \rho} = .72 \dots \tag{27.36}$$

For negative  $\tau$  the sum (27.35) is the lower bound on the sum (27.25), so  $\hat{D}$  is a lower bound on  $D_H$ .

From a general perspective the analysis of circle maps thermodynamics has revealed the fact that physically interesting dynamical systems often exhibit mixtures of hyperbolic and marginal stabilities. In such systems there are orbits that

$\tau/2$	$Z_n(\tau/2)/Z_{n-1}(\tau/2)$
0	2
1	3
2	$(5 + \sqrt{17})/2$
3	7
4	$(5 + \sqrt{17})/2$
5	$7 + 4\sqrt{6}$
6	26.20249...

Table 27.2: Partition function sum rules for the Farey model.

stay ‘glued’ arbitrarily close to stable regions for arbitrarily long times. This is a generic phenomenon for Hamiltonian systems, where elliptic islands of stability coexist with hyperbolic homoclinic webs. Thus the considerations of chapter 24 are important also in the analysis of renormalization at the onset of chaos.

### Résumé

The mode locking problem, and the quasiperiodic transition to chaos offer an opportunity to use cycle expansions on hierarchical structures in parameter space: this is not just an application of the conventional thermodynamic formalism, but offers a clue on how to extend universality theory from local scalings to global quantities.

### Commentary

**Remark 27.1** The physics of circle maps. Mode-locking phenomenology is reviewed in ref. [27.5], a more theoretically oriented discussion is contained in ref. [27.3]. While representative of dissipative systems we may also consider circle maps as a crude approximation to Hamiltonian local dynamics: a typical island of stability in a Hamiltonian 2 – dimensional map is an infinite sequence of concentric KAM tori and chaotic regions. In the crudest approximation, the radius can here be treated as an external parameter  $\Omega$ , and the angular motion can be modeled by a map periodic in the angular variable [27.8, 27.9]. By losing all of the ‘island-within-island’ structure of real systems, circle map models skirt the problems of determining the symbolic dynamics for a realistic Hamiltonian system, but they do retain some of the essential features of such systems, such as the golden mean renormalization [13.5, 27.8] and non-hyperbolicity in form of sequences of cycles accumulating toward the borders of stability. In particular, in such systems there are orbits that stay “glued” arbitrarily close to stable regions for arbitrarily long times. As this is a generic phenomenon in physically interesting dynamical systems, such as the Hamiltonian systems with coexisting elliptic islands of stability and hyperbolic homoclinic webs, development of good computational techniques is here of utmost practical importance.

**Remark 27.2** Critical mode-locking set The fact that mode-lockings completely fill the unit interval at the critical point has been proposed in refs. [27.3, 27.10]. The proof that the set of irrational windings is of zero Lebesgue measure is given in ref. [27.11].

**Remark 27.3** Counting noise for Farey series. The number of rationals in the Farey series of order  $Q$  is  $\phi(Q)$ , which is a highly irregular function of  $Q$ : incrementing  $Q$  by 1 increases  $\Phi(Q)$  by anything from 2 to  $Q$  terms. We refer to this fact as the “Euler noise.”

The Euler noise poses a serious obstacle for numerical calculations with the Farey series partitionings; it blocks smooth extrapolations to  $Q \rightarrow \infty$  limits from finite  $Q$  data. While this in practice renders inaccurate most Farey-sequence partitioned averages, the finite  $Q$  Hausdorff dimension estimates exhibit (for reasons that we do not understand) surprising numerical stability, and the Farey series partitioning actually yields the *best* numerical value of the Hausdorff dimension (27.25) of any methods used so far; for example the computation in ref. [27.12] for critical sine map (27.1), based on  $240 \leq Q \leq 250$  Farey series partitions, yields  $D_H = .87012 \pm .00001$ . The quoted error refers to the variation of  $D_H$  over this range of  $Q$ ; as the computation is not asymptotic, such numerical stability can underestimate the actual error by a large factor.

**Remark 27.4** Farey tree presentation function. The Farey tree rationals can be generated by backward iterates of  $1/2$  by the Farey presentation function [27.13]:

$$\begin{aligned} f_0(x) &= x/(1-x) & 0 \leq x < 1/2 \\ f_1(x) &= (1-x)/x & 1/2 < x \leq 1. \end{aligned} \tag{27.37}$$

The Gauss shift (27.7) corresponds to replacing the binary Farey presentation function branch  $f_0$  in (27.37) by an infinity of branches

$$\begin{aligned} f_a(x) &= f_1 \circ f_0^{(a-1)}(x) = \frac{1}{x} - a, & \frac{1}{a-1} < x \leq \frac{1}{a}, \\ f_{ab\dots c}(x) &= f_c \circ \dots \circ f_b \circ f_a(x). \end{aligned} \tag{27.38}$$

A rational  $x = [a_1, a_2, \dots, a_k]$  is annihilated by the  $k$ th iterate of the Gauss shift,  $f_{a_1 a_2 \dots a_k}(x) = 0$ . The above maps look innocent enough, but note that what is being partitioned is not the dynamical space, but the parameter space. The flow described by (27.37) and by its non-trivial circle-map generalizations will turn out to be a *renormalization group* flow in the function space of dynamical systems, not an ordinary flow in the state space of a particular dynamical system.

The Farey tree has a variety of interesting symmetries (such as “flipping heads and tails” relations obtained by reversing the order of the continued-fraction entries) with as yet unexploited implications for the renormalization theory: some of these are discussed in ref. [27.4].

An alternative labeling of Farey denominators has been introduced by Knauf [27.6] in context of number-theoretical modeling of ferromagnetic spin chains: it allows for a number of elegant manipulations in thermodynamic averages connected to the Farey tree hierarchy.

**Remark 27.5** Circle map renormalization The idea underlying golden mean renormalization goes back to Shenker [27.9]. A renormalization group procedure was formulated in refs. [27.7, 27.14], where moreover the uniqueness of the relevant eigenvalue is claimed. This statement has been confirmed by a computer-assisted proof [27.15], and in the following we will always assume it. There are a number of experimental evidences for local universality, see refs. [27.16, 27.17].

On the other side of the scaling tale, the power law scaling for harmonic fractions (discussed in refs. [27.2, 27.4]) is derived by methods akin to those used in describing intermittency [27.21]:  $1/Q$  cycles accumulate toward the edge of  $0/1$  mode-locked interval, and as the successive mode-locked intervals  $1/Q$ ,  $1/(Q-1)$  lie on a parabola, their differences are of order  $Q^{-3}$ .

**Remark 27.6** Farey series and the Riemann hypothesis The Farey series thermodynamics is of a number theoretical interest, because the Farey series provide uniform coverings of the unit interval with rationals, and because they are closely related to the deepest problems in number theory, such as the Riemann hypothesis [27.22, 27.23]. The distribution of the Farey series rationals across the unit interval is surprisingly uniform - indeed, so uniform that in the pre-computer days it has motivated a compilation of an entire handbook of Farey series [27.24]. A quantitative measure of the non-uniformity of the distribution of Farey rationals is given by displacements of Farey rationals for  $P_i/Q_i \in \mathcal{F}_Q$  from uniform spacing:

$$\delta_i = \frac{i}{\Phi(Q)} - \frac{P_i}{Q_i}, \quad i = 1, 2, \dots, \Phi(Q)$$

The Riemann hypothesis states that the zeros of the Riemann zeta function lie on the  $s = 1/2 + ir$  line in the complex  $s$  plane, and would seem to have nothing to do with physicists' real mode-locking widths that we are interested in here. However, there is a real-line version of the Riemann hypothesis that lies very close to the mode-locking problem. According to the theorem of Franel and Landau [27.25, 27.22, 27.23], the Riemann hypothesis is equivalent to the statement that

$$\sum_{Q_i \leq Q} |\delta_i| = o(Q^{\frac{1}{2} + \epsilon})$$

for all  $\epsilon$  as  $Q \rightarrow \infty$ . The mode-lockings  $\Delta_{P/Q}$  contain the necessary information for constructing the partition of the unit interval into the  $\ell_i$  covers, and therefore implicitly contain the  $\delta_i$  information. The implications of this for the circle-map scaling theory have not been worked out, and is not known whether some conjecture about the thermodynamics of irrational windings is equivalent to (or harder than) the Riemann hypothesis, but the danger lurks.

**Remark 27.7** Farey tree partitioning. The Farey tree partitioning was introduced in refs. [27.26, 27.27, 27.4] and its thermodynamics is discussed in detail in refs. [27.12, 27.13]. The Farey tree hierarchy of rationals is rather new, and, as far as we are aware, not previously studied by number theorists. It is appealing both from the experimental and from the golden-mean renormalization point of view, but it has a serious drawback of lumping together mode-locking intervals of wildly different sizes on the same level of the Farey tree.

**Remark 27.8** Local and global universality. Numerical evidences for global universal behavior have been presented in ref. [27.3]. The question was reexamined in ref. [27.12], where it was pointed out how a high-precision numerical estimate is in practice very hard to obtain. It is not at all clear whether this is the optimal global quantity to test but at least the Hausdorff dimension has the virtue of being independent of how one partitions mode-lockings and should thus be the same for the variety of thermodynamic averages in the literature.

The formula (27.30), linking local to global behavior, was proposed in ref. [27.1].

The derivation of (27.30) relies only on the following aspects of the “hyperbolicity conjecture” of refs. [27.4, 27.18, 27.19, 27.20]:

1. *limits* for Shenker  $\delta$ 's exist and are universal. This should follow from the renormalization theory developed in refs. [27.7, 27.14, 27.15], though a general proof is still lacking.
2.  $\delta_p$  grow exponentially with  $n_p$ , the length of the continued fraction block  $p$ .
3.  $\delta_p$  for  $p = a_1 a_2 \dots n$  with a large continued fraction entry  $n$  grows as a power of  $n$ . According to (27.14),  $\lim_{n \rightarrow \infty} \delta_p \propto n^3$ . In the calculation of ref. [27.1] the explicit values of the asymptotic exponents and prefactors were not used, only the assumption that the growth of  $\delta_p$  with  $n$  is not slower than a power of  $n$ .

**Remark 27.9** Farey model. The Farey model (27.33) has been proposed in ref. [27.12]; though it might seem to have been pulled out of a hat, the Farey model is as sensible description of the distribution of rationals as the periodic orbit expansion (27.26).

**Remark 27.10** Symbolic dynamics for Hamiltonian rotational orbits. The rotational codes of ref. [27.37] are closely related to those for maps with a natural angle variable, for example for circle maps [27.34, 27.36] and cat maps [27.38]. Ref. [27.37] also offers a systematic rule for obtaining the symbolic codes of “islands around islands” rotational orbits [27.40]. These correspond, for example, to orbits that rotate around orbits that rotate around the elliptic fixed point; thus they are defined by a sequence of rotation numbers.

A different method for constructing symbolic codes for “islands around islands” was given in refs. [27.43, 27.41]; however in these cases the entire set of orbits in an island was assigned the same sequence and the motivation was to study the transport implications for chaotic orbits outside the islands [27.40, 27.42].

## Exercises

- 27.1. **Mode-locked intervals.** Check that when  $k \neq 0$  the interval  $\Delta_{P/Q}$  have a non-zero width (look for instance at simple fractions, and consider  $k$  small). Show that for small  $k$  the width of  $\Delta_{0/1}$  is an increasing function of  $k$ .

27.2. **Bounds on Hausdorff dimension.** By making use of the bounds (27.17) show that the Hausdorff dimension for critical mode lockings may be bounded by

$$2/3 \leq D_H \leq .9240 \dots$$

27.3. **Farey model sum rules.** Verify the sum rules reported in table 27.2. An elegant way to get a number of sum rules for the Farey model is by taking into account an lexical ordering introduced by Contucci and Knauf, see ref. [27.28].

27.4. **Metric entropy of the Gauss shift.** Check that the Lyapunov exponent of the Gauss map (27.7) is given by  $\pi^2/6 \ln 2$ . This result has been claimed to be relevant in the discussion of “mixmaster” cosmologies, see ref. [27.30].

27.5. **Refined expansions.** Show that the above estimates can be refined as follows:

$$F(z, 2) \sim \zeta(2) + (1-z) \log(1-z) - (1-z)$$

and

$$F(z, s) \sim \zeta(s) + \Gamma(1-s)(1-z)^{s-1} - S(s)(1-z)$$

for  $s \in (1, 2)$  ( $S(s)$  being expressed by a converging sum). You may use either more detailed estimate for  $\zeta(s, a)$  (via Euler summation formula) or keep on subtracting leading contributions [27.31].

27.6.  $j_n$  and  $\alpha_{cr}$ . Look at the integration region and how it scales by plotting it for increasing values of  $n$ .

27.7. **Estimates of the Riemann zeta function.** Try to approximate numerically the Riemann zeta function for  $s = 2, 4, 6$  using different acceleration algorithms: check your results with refs. [27.32, 27.33].

27.8. **Farey tree and continued fractions I.** Consider the Farey tree presentation function  $f : [0, 1] \mapsto [0, 1]$ , such that if  $I = [0, 1/2)$  and  $J = [1/2, 1]$ ,  $f_I = x/(1-x)$  and  $f_J = (1-x)/x$ . Show that the corresponding induced map is the Gauss map  $g(x) = 1/x - [1/x]$ .

27.9. **Farey tree and continued fraction II. (Lethal weapon II).** Build the simplest piecewise linear approximation to the Farey tree presentation function (hint: substitute first the rightmost, hyperbolic branch with a linear one): consider then the spectral determinant of the induced map  $\hat{g}$ , and calculate the first two eigenvalues besides the probability conservation one. Compare the results with the rigorous bound deduced in ref. [24.17].

## References

- [27.1] P. Cvitanović, G.H. Gunaratne and M. Vinson, *Nonlinearity* **3** (1990)
- [27.2] K. Kaneko, *Prog. Theor. Phys.* **68**, 669 (1982); **69**, 403 (1983); **69**, 1427 (1983)
- [27.3] M.H. Jensen, P. Bak, T. Bohr, *Phys. Rev. Lett.* **50**, 1637 (1983); *Phys. Rev. A* **30**, 1960 (1984); P. Bak, T. Bohr and M.H. Jensen, *Physica Scripta* **T9**, 50 (1985)
- [27.4] P. Cvitanović, B. Shraiman and B. Söderberg, *Physica Scripta* **32**, 263 (1985).
- [27.5] J.A. Glazier and A. Libchaber, *IEEE Trans. Circ. Syst.*, **35**, 790 (1988)
- [27.6] A. Knauf, “On a ferromagnetic spin chain,” *Commun. Math. Phys.* **153**, 77 (1993).
- [27.7] M.J. Feigenbaum, L.P. Kadanoff, S.J. Shenker, *Physica* **5D**, 370 (1982)
- [27.8] S.J. Shenker and L.P. Kadanoff, *J. Stat. Phys.* **27**, 631 (1982)
- [27.9] S.J. Shenker, *Physica* **5D**, 405 (1982)
- [27.10] O.E. Lanford, *Physica* **14D**, 403 (1985)

- [27.11] G. Swiatek, *Commun. Math. Phys.* **119**, 109 (1988)
- [27.12] R. Artuso, P. Cvitanović and B.G. Kenny, *Phys. Rev.* **A39**, 268 (1989); P. Cvitanović, in R. Gilmore (ed), *Proceedings of the XV International Colloquium on Group Theoretical Methods in Physics*, (World Scientific, Singapore, 1987)
- [27.13] M.J. Feigenbaum, *J. Stat. Phys.* **52**, 527 (1988)
- [27.14] S. Ostlund, D.A. Rand, J. Sethna and E. Siggia, *Physica* **D 8**, 303 (1983).
- [27.15] B.D. Mestel, Ph.D. Thesis (U. of Warwick 1985).
- [27.16] J. Stavans, F. Heslot and A. Libchaber, *Phys. Rev. Lett.* **55**, 569 (1985)
- [27.17] E.G. Gwinn and R.M. Westervelt, *Phys. Rev. Lett.* **59**, 157 (1987)
- [27.18] O.E. Lanford, in M. Mebkhout and R. S enior, eds., *Proc. 1986 IAMP Conference in Mathematical Physics* (World Scientific, Singapore 1987); D.A. Rand, *Proc. R. Soc. London A* **413**, 45 (1987); *Nonlinearity* **1**, 78 (1988)
- [27.19] S.-H. Kim and S. Ostlund, *Physica* **D 39**, 365, (1989)
- [27.20] M.J. Feigenbaum, *Nonlinearity* **1**, 577 (1988)
- [27.21] Y. Pomeau and P. Manneville, *Commun. Math. Phys.* **74**, 189 (1980); P. Manneville, *J. Phys. (Paris)* **41**, 1235 (1980)
- [27.22] H.M. Edwards, *Riemann’s Zeta Function* (Academic, New York 1974)
- [27.23] E.C. Titchmarsh, *The Theory of Riemann Zeta Function* (Oxford Univ. Press, Oxford 1951); chapter XIV.
- [27.24] E.H. Neville, *Roy. Soc. Mathematical Tables* (Cambridge Univ. Press, Cambridge 1950)
- [27.25] J. Franel and E. Landau, *G ottinger Nachr.* 198 (1924)
- [27.26] G. T. Williams and D. H. Browne, *Amer. Math. Monthly* **54**, 534 (1947)
- [27.27] P. Cvitanović and J. Myrheim, *Phys. Lett.* **A94**, 329 (1983); *Commun. Math. Phys.* **121**, 225 (1989)
- [27.28] P. Contucci and A. Knauf, *Forum Math.* **9**, 547 (1997)
- [27.29] G.H. Hardy and E.M. Wright, *Theory of Numbers* (Oxford Univ. Press, Oxford 1938)
- [27.30] A. Csord as and P. Sz epfalusy, *Phys. Rev. A* **40**, 2221 (1989) and references therein.
- [27.31] P. Dahlqvist, unpublished notes.
- [27.32] D. Levin, *Inter. J. Computer Math.* **B3**, 371 (1973).

- [27.33] N. Osada, *SIAM J. Numer. Anal.* **27**, 178 (1990).
- [27.34] P. Veerman, "Symbolic dynamics and rotation numbers," *Phys. A* **134**, 543 (1986).
- [27.35] J.J.P. Veerman and F.M. Tangerman. "Intersection properties of invariant manifolds in certain twist maps," *Comm. Math. Phys.* **139**, 245 (1991).
- [27.36] W.-M. Zheng, "Symbolic dynamics for the circle map," *Int. J. Mod. Phys. B* **5**, 481 (1991).
- [27.37] H.R. Dullin, J.D. Meiss and D.G. Sterling, "Symbolic codes for rotational orbits,"  
[arXiv:nlin.CD/0408015](https://arxiv.org/abs/nlin.CD/0408015).
- [27.38] I.C. Percival and F. Vivaldi. "A linear code for the sawtooth and cat maps," *Physica D* **27**, 373 (1987).
- [27.39] I.C. Percival and F. Vivaldi. "Arithmetical properties of strongly chaotic motion," *Physica D* **25**, 105 (1987).
- [27.40] J.D. Meiss, "Class renormalization: Islands around islands," *Phys. Rev. A* **34**, 2375 (1986).
- [27.41] V. Afraimovich, A. Maass, and J. Uras. "Symbolic dynamics for sticky sets in Hamiltonian systems," *Nonlinearity* **13**, 617 (2000).
- [27.42] J.D. Meiss and E. Ott. "Markov tree model of transport in area preserving maps," *Physica D* **20**, 387 (1986).
- [27.43] Y. Aizawa. "Symbolic dynamics approach to the two-D chaos in area-preserving maps," *Prog. Theor. Phys.* **71**, 1419 (1984).
- [27.44] M. Yampolsky, "On the eigenvalues of a renormalization operator," *Nonlinearity* **16**, 1565 (2003).